



Proteomic analysis of the reduction and resistance mechanisms of *Shewanella oneidensis* MR-1 under long-term hexavalent chromium stress

Haiyin Gang^{a,b}, Changye Xiao^{b,c}, Yong Xiao^{b,c,*}, Weifu Yan^b, Rui Bai^{b,c}, Rui Ding^{b,c}, Zhaohui Yang^{a,*}, Feng Zhao^{b,c}

^a Key Laboratory of Environmental Biology and Pollution Control, Ministry of Education, College of Environmental Science and Engineering, Hunan University, Changsha 410082, China

^b CAS Key Laboratory of Urban Pollutant Conversion, Institute of Urban Environment, Chinese Academy of Sciences, Xiamen 361021, China

^c University of Chinese Academy of Sciences, Beijing 100049, China

ARTICLE INFO

Handling Editor: Guo-ping Sheng

Keywords:

Shewanella oneidensis MR-1
Hexavalent chromium
Long-term acclimatization
Permanent effect
Short-term stimulus

ABSTRACT

Hexavalent chromium [Cr(VI)] is a priority heavy metal pollutant causing a series of environmental issues, and bio-reduction of Cr(VI) to trivalent chromium can remarkably decrease the environmental risk of Cr(VI). The reduction and resistance abilities of microorganisms to Cr(VI) can be dramatically improved by acclimatization. In the present study, we collected *Shewanella oneidensis* MR-1 from a 120-day acclimatization by increasing Cr(VI) concentration in the culture media to investigate its adaptation mechanisms under long-term Cr(VI) stress at the proteome level. Tandem mass tag-based quantitative proteomic analysis was performed to study the differences between 9 collected samples. A total of 2500 proteins were quantified from 2723 identified protein groups. Bioinformatics analysis showed that the differentially expressed proteins after the 120-day Cr(VI) acclimatization were mostly related to flagellar assembly, ribosomes, transport, sulfur metabolism, and energy metabolism. The findings of this study present novel insights into the molecular mechanisms for the reduction and resistance of *S. oneidensis* MR-1 responding to long-term Cr(VI) stress at the proteome level.

1. Introduction

Chromium, an important heavy metal, has been widely used in industry, such as electroplating, wood preservation, production of steel and alloy, leather tanning, and pigmentation (Dhal et al., 2013). Hexavalent chromium [Cr(VI)] causes many serious environmental issues and remarkably threatens all kinds of lives, including the lives of animals, plants, microorganisms and humans, due to its high toxicity, mutagenicity and carcinogenicity. Therefore, it is essential to address Cr(VI) contamination by efficient, economical and ecological methods. At present, the most efficient way to treat Cr(VI) contamination is by converting Cr(VI) into a much less toxic trivalent chromium [Cr(III)]. Some studies have focused on Cr(VI) reduction and detoxication by employing various chemical or biological approaches, and microbiological reduction is a more promising strategy for the remediation of various Cr(VI)-contaminated environments (Alencar et al., 2017; Chai et al., 2018; Cheung and Gu, 2007; Dhal et al., 2013; Pradhan et al., 2017). Wang et al. (2016) used microbial fuel cells for the remediation of Cr(VI)-contaminated soils.

Microorganisms' capacities for reduction and/or resistance to

pollutants can be achieved by long-term acclimatization. For example, the removal efficiency of a high concentration of sulfamethazine antibiotics could be promoted by acclimatizing activated sludge in reactors fed with increasing sulfamethazine antibiotics (Yang et al., 2015). Chen et al. (2006) investigated the effect of microorganism acclimatization on enhanced phosphorus biological removal from wastewater. The reduction and resistance abilities of microorganisms to Cr(VI) can also be dramatically improved by long-term acclimatization.

Shewanella oneidensis MR-1, a model strain of dissimilatory metal reduction bacteria, is capable of reducing Cr(VI) to Cr(III) aerobically or anaerobically (Belchik et al., 2011; Meng et al., 2018). The mechanisms of *S. oneidensis* MR-1 for resisting or reducing Cr(VI) have been reported extensively (Bencheikh-Latmani et al., 2005; Brown et al., 2006; Wang et al., 2014). *S. oneidensis* MR-1 reduces Cr(VI) aerobically using a soluble reductase of NADH or endogenous electron reserves as electron donor, while the anaerobic reduction of Cr(VI) relates to the electron transport system involving membrane cytochromes (Wang and Shen, 1995). However, these findings are mostly based on short-term exposure of *S. oneidensis* MR-1 to low-concentration Cr(VI), and no study has focused on the adaptation mechanisms of bacteria in the Cr(VI)

* Corresponding authors.

E-mail addresses: yxiao@iue.ac.cn (Y. Xiao), yzh@hnu.edu.cn (Z. Yang).

<https://doi.org/10.1016/j.envint.2019.03.016>

Received 2 November 2018; Received in revised form 25 January 2019; Accepted 7 March 2019

0160-4120/© 2019 The Authors. Published by Elsevier Ltd. This is an open access article under the CC BY license (<http://creativecommons.org/licenses/by/4.0/>).

environment aiming at an engineering application. Therefore, the molecular mechanisms for reduction and resistance of bacteria responding to the stress from long-term high-concentration Cr(VI), i.e., the acclimatization process, have never been clarified.

Proteomics is quite a powerful tool to explore the cellular molecular mechanism of organisms responding to environmental stress by analyzing differentially expressed proteins (DEPs). In the present study, we analyzed the proteome of *S. oneidensis* MR-1 after 120-day Cr(VI) exposure to determine the response mechanism of MR-1 against long-term Cr(VI) exposure. The DEPs were identified by high-resolution liquid chromatography-tandem mass spectrometry (LC-MS/MS). The results will further shed light on the molecular mechanism for resistance and reduction in MR-1 under long-term Cr(VI) exposure at the proteomic level, which can help us to make effective bioremediation and environmental risk assessments through long-term acclimatization.

2. Materials and methods

2.1. Bacterial strains and Cr(VI) treatment

The strain used in this study was the *S. oneidensis* strain MR-1, which was cultured in Luria-Bertani (LB) broth without and with Cr(VI) for 120 days and was designated D120N and D120Cr, respectively. The LB medium contains tryptone (10 g/L), yeast extract (5 g/L) and NaCl (10 g/L) (pH 7.0). The experimental strains were aerobically grown at 30 °C in 250-mL Erlenmeyer flasks containing a 100-mL LB medium by shaking at 150 rpm. The inoculation ratio was 1.0%. Cr(VI) stock solution was 100 mM K₂CrO₄ solution. The final concentration of Cr(VI) was 312 mg/L in D120Cr(+), and no Cr(VI) was added in D120N and D120Cr(−) (Fig. S1). The cell samples of D120Cr(+), D120N and D120Cr(−) were collected for protein processing after 8, 5 and 6 h, respectively. Each treatment was prepared in triplicate.

2.2. Protein extraction and digestion

The extraction and digestion of proteins were based on the published method (Wang et al., 2017). Samples were sonicated three times on ice using a high-intensity ultrasonic processor (JY92-IIN, Scientz, China) in four volumes of lysis buffer (8 M urea, 1% v/v Triton-100, 10 mM dithiothreitol, 1% v/v protease inhibitor cocktail and 2 mM ethylene diamine tetraacetic acid). The remaining debris was removed by centrifugation at 20,000g at 4 °C for 10 min. Finally, the supernatant was collected, and the protein was precipitated with cold 20% w/v trichloroacetic acid for 2 h at 4 °C. After centrifugation at 12,000 g at 4 °C for 3 min, the supernatant was discarded. The remaining precipitate was washed three times with cold acetone. The protein was redissolved in 8 M urea, and the protein concentration was determined with a BCA kit (Beyotime, China) according to the manufacturer's instructions.

For digestion, the protein solution was reduced with 5 mM dithiothreitol for 30 min at 56 °C and alkylated with 11 mM iodoacetamide for 15 min at room temperature in darkness. The protein sample was then diluted by adding 100 mM TEAB to urea concentration < 2 M. Finally, trypsin (Promega, USA) was added at a 1:50 trypsin-to-protein mass ratio for the first digestion overnight at 37 °C and 1:100 trypsin-to-protein mass ratio for a second 4 h-digestion.

2.3. TMT labeling and HPLC fractionation

The digested samples were desalted by the Strata X C18 SPE column (Phenomenex, USA) and vacuum freeze-dried. Peptides were reconstituted in 0.5 M TEAB and labeled using the TMT-10plex Kit (Thermo Fisher Scientific) according to the manufacturer's instructions. All samples were pooled and vacuum freeze-dried. The labeled peptide mixtures were fractionated into fractions by high pH reverse-phase HPLC using the Agilent 300Extend C18 column (5 μm particles, 4.6 mm

ID, 250 mm length). The peptides were combined into 18 fractions and vacuum freeze-dried.

2.4. LC-MS/MS analysis

LC – MS/MS analysis was performed using the EASY-nLC 1000 UPLC system (Thermo Fisher Scientific) coupled with a Q-Exactive Hybrid Quadrupole-Orbitrap mass spectrometer (Thermo Fisher Scientific) with a nanospray ionization (NSI) source. A data-dependent procedure that alternated between one MS scan (70,000 resolving power) and 20 MS/MS (30,000 resolving power) scans with 30 s dynamic exclusion.

2.5. Database search and bioinformatic analysis

The resulting MS/MS data were processed using the Maxquant search engine (v.1.5.2.8). The obtained peptide sequences were searched against the UniProt *Shewanella oneidensis* (strain MR-1) (4068 sequences) database concatenated with a reverse decoy database. The false discovery rate (FDR) was adjusted to < 0.01. The DEPs were identified only if the normalized fold change was higher than 2.0 (up-regulated) or < 0.5 (downregulated). The DEPs were annotated into three categories based on gene ontology (GO) terms, i.e., biological process, cellular component and molecular function. The protein pathway was annotated using the Kyoto Encyclopedia of Genes and Genomes (KEGG) database. The protein domain function was defined by InterProScan based on the protein sequence alignment method (<http://www.ebi.ac.uk/interpro/>). We used WoLF PSORT (a subcellular localization prediction software) to predict subcellular localization. Enrichment analysis was conducted for the GO terms, the KEGG pathway and the protein domain using the Database for Annotation, Visualization and Integrated Discovery. The statistically significant enrichments were identified using Fisher's exact test with Benjamini-Hochberg's corrected *P* value < 0.05. Hierarchical clustering analysis was conducted for the DEPs based on the significant enrichments using the “heatmap.2” function from the “gplots” R package. The proteomics analysis in our research was supported by Jingjie PTM BioLabs (Hangzhou, China).

3. Results

3.1. Protein identification and comparison

Up to 2723 proteins were identified by proteomics analysis, of which 2500 proteins were quantified in all samples, the mass error of the whole identified peptides and the repeatability of samples are shown in Figs. S2 and S3. A quantitative ratio of higher than 2 was considered to be an upregulation, whereas that < 0.5 was considered to be a downregulation. All quantifiable proteins with increased (≥ 2 -fold) and decreased (≤ 0.5 -fold) expression levels are listed in Table S1 and S2 (*P* < 0.05).

As shown in Fig. 1A, compared with D120N, 239 DEPs were induced in D120Cr(−), including 63 upregulated proteins, such as the MSHA major pilin subunit MshA, and 176 downregulated proteins, such as the extracellular iron oxide respiratory system outer membrane component MtrB; 509 DEPs were identified from D120Cr(+), including 315 up-regulated proteins, such as the FMN-binding heme iron utilization protein HmuZ and the ABC-type heme uptake system substrate-binding component HmuB, and 194 downregulated proteins, such as the extracellular iron oxide respiratory system outer membrane component MtrB. Compared with D120Cr(−), D120Cr(+) induced 447 DEPs: 397 upregulated expressed proteins and 50 downregulated expressed proteins. The Venn diagrams showed the number of common and unique upregulated/downregulated or all expressed proteins in all cases (Figs. 1B, C and S4).

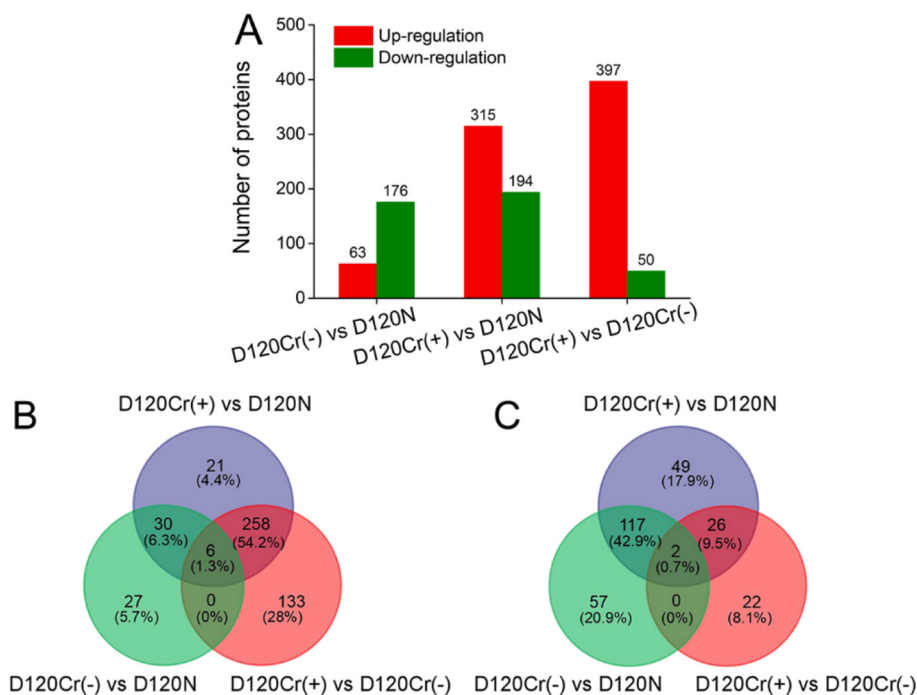


Fig. 1. Number of differentially expressed proteins (A) and Venn diagram showing the common and unique upregulated (B) or downregulated (C) expressed proteins.

3.2. Functional characterization of differentially expressed proteins

These DEPs were classified according to their subcellular location (Fig. 2). For D120Cr(-) versus D120N, 48%, 24% and 14% of DEPs were located in the cytoplasm, periplasmic and outer membrane, respectively. For D120Cr(+) versus D120N, 52% of DEPs were located in the cytoplasm, 27% were located in the periplasmic, and 10% were in the outer membrane. For D120Cr(+) versus D120Cr(-), 54% of DEPs were located in the cytoplasm, 28% were located in the periplasmic, and 8% were located in the outer membrane. The DEPs mainly were located in the cytoplasm, periplasmic and outer membrane in three cases, meaning that Cr(VI) resistance and the reduction of *S. oneidensis* MR-1 were mainly induced by changes in the cytoplasm, periplasmic and outer membrane.

Based on the GO analysis tool, the biological functions affected by DEPs were classified to the cellular component, molecular function, and biological process. The affected biological functions and the number of proteins in D120Cr(-) and D120N, D120Cr(+) and D120N and in D120Cr(+) and D120Cr(-) were analyzed and compared. The mainly affected biological functions and the amount of related proteins in all comparison groups are summarized in Table 1 and Fig. 3. The results show that these DEPs were mainly involved in the organelle, membrane, cell, catalytic activity, binding, transporter activity, structural molecule activity, metabolic process, single-organism process, localization and cellular process. Almost all DEPs have certain direct or indirect interactions with other proteins in each case (Figs. 4 and S5). Moreover, some proteins associated with streptomycin biosynthesis,

beta-lactam resistance, flagellar assembly, and ribosomes were found to be especially highly clustered among the intensive interaction networks (Fig. S6).

3.3. Functional enrichment of differentially quantified proteins and clustering for protein groups

To investigate the functional differences in upregulated and down-regulated proteins, the quantified proteins were analyzed separately for GO terms (molecular function, cellular component, and biological process), the protein KEGG pathway and domain enrichment as well as for enrichment-based clustering (Figs. 5, S7, S8 and S9). The proteins were significantly enriched to indicate the nature of the DEPs in each comparison group.

GO enrichment analysis of the DEPs was performed to classify the biological processes, molecular functions, and cellular components in Figs. 5 (A, B and C) and S7. For D120Cr(-) vs. D120N, the 63 up-regulated proteins were mainly enriched in oxidoreductase activity (GO:0016702), dioxygenase activity (GO: 0051213), and organic acid catabolic process (GO: 0016054); meanwhile, the 176 downregulated proteins were mainly related to sulfate assimilation (GO: 0000103) and transport (GO: 0006810). For D120Cr(+) vs. D120N, the upregulated proteins were mainly involved in the structural molecule activity (GO: 0005198), 2 iron-2 sulfur cluster binding (GO: 0051537) and cell motility (GO: 0048870); meanwhile the downregulated proteins were mainly significantly enriched in the oxidation-reduction process (GO: 0055114), sulfate assimilation (GO: 0000103) and transport (GO:

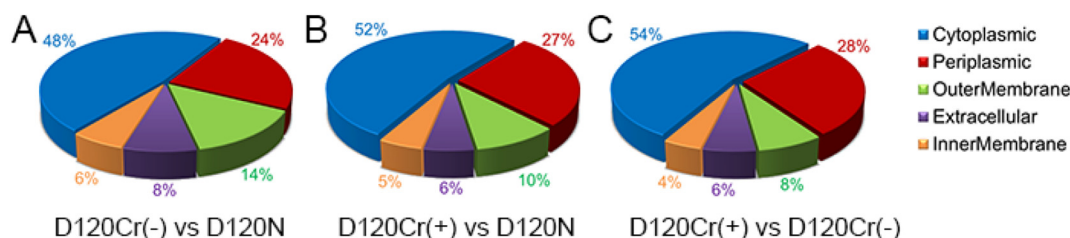


Fig. 2. Subcellular location of differentially expressed proteins.

Table 1
Gene ontology (GO) distribution of differentially expressed proteins.

GO Terms Level 1	GO Terms Level 2	No. proteins (%)		
		D120Cr(−) vs D120N	D120Cr(+) vs D120N	D120Cr(+) vs D120Cr(−)
Cellular component	Organelle	1 (2%)	24 (15%)	43 (22%)
	Membrane	33 (57%)	60 (37%)	44 (23%)
	Macromolecular complex	3 (5%)	16 (10%)	35 (18%)
	Cell	21 (36%)	62 (38%)	73 (37%)
Molecular function	Catalytic activity	99 (51%)	164 (41%)	113 (34%)
	Binding	58 (30%)	143 (35%)	115 (35%)
	Structural molecule activity	2 (1%)	18 (4%)	37 (11%)
	Transporter activity	17 (9%)	33 (8%)	19 (6%)
Biological process	Metabolic process	76 (32%)	153 (26%)	126 (25%)
	Single-organism process	55 (23%)	133 (22%)	97 (20%)
	Localization	31 (13%)	69 (12%)	54 (11%)
	Cellular process	49 (21%)	144 (24%)	134 (27%)

0006810). For D120Cr(+) vs. D120Cr(−), the upregulated proteins were mainly associated with structural molecule activity (GO: 0005198), iron ion binding (GO: 0005506), peptide metabolic process (GO: 0006518), translation (GO: 0006412) and cell motility (GO: 0048870); the downregulation proteins were mainly enriched in transport (GO: 0006810), organic acid transport (GO: 0015849) and

metal ion homeostasis (GO: 0055065).

The KEGG pathway enrichment results are shown in Figs. 5D and S8. For D120Cr(−) vs. D120N, the upregulated expressed proteins were significantly enriched in beta-lactam resistance (ko01501), cationic antimicrobial peptide (CAMP) resistance (ko01503), phenylalanine metabolism (ko00360) and tyrosine metabolism (ko00350); the

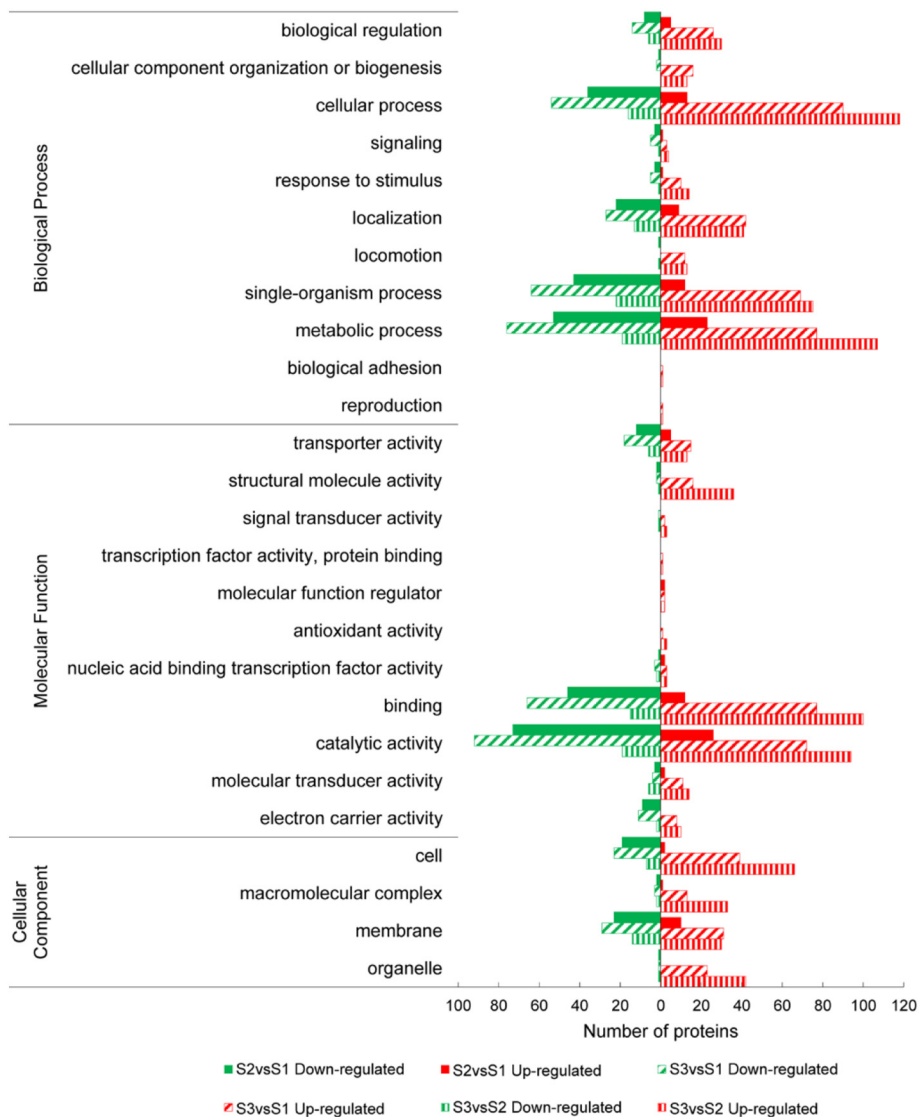


Fig. 3. Functional category distribution of differentially expressed proteins. S1, D120N; S2, D120Cr(−); S3, D120Cr(+).

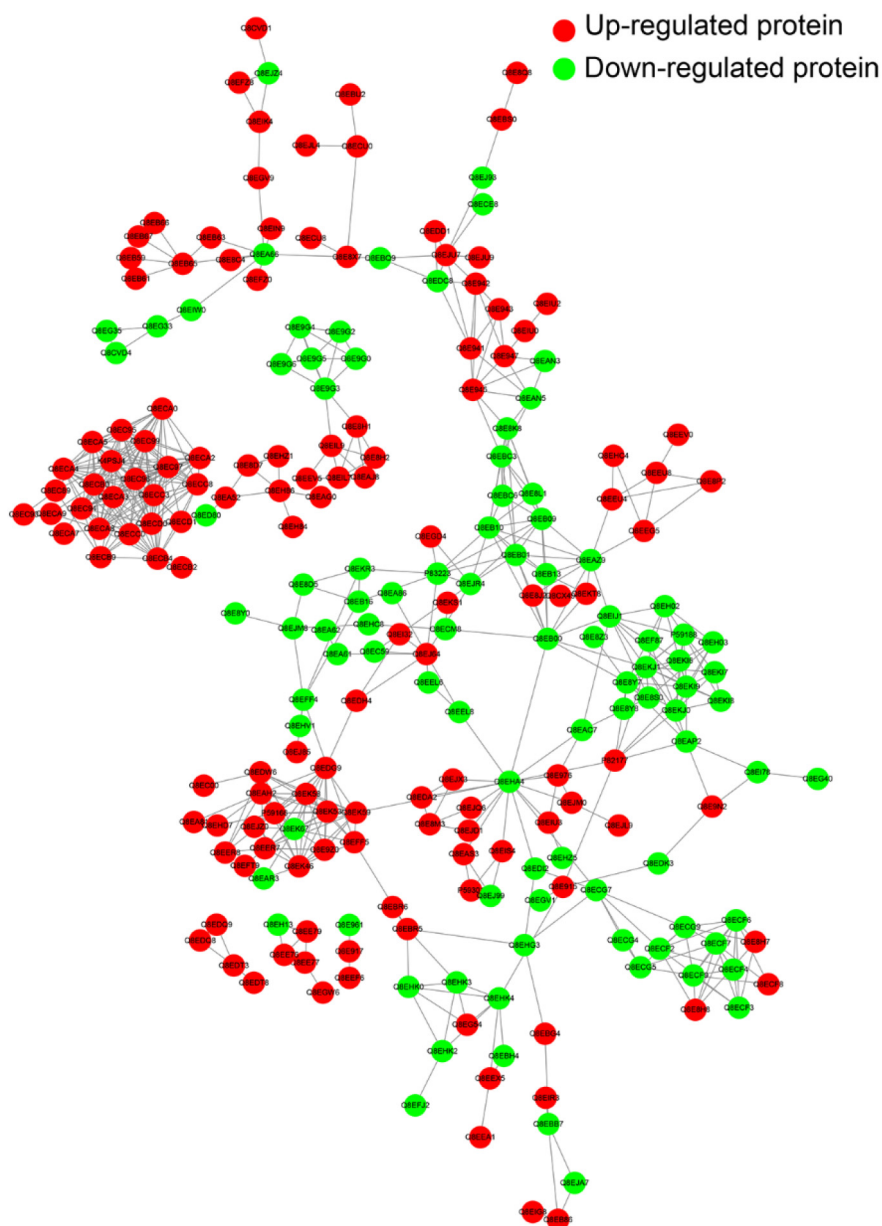


Fig. 4. The protein and protein interaction networks of all differentially expressed proteins in D120Cr(+) vs D120N.

downregulated expressed proteins were mainly enriched in sulfur metabolism (ko00920) and ATP-binding cassette (ABC) transporters (ko02010). For D120Cr(+) vs. D120N, the upregulated DEPs were enriched in flagellar assembly (ko02040), CAMP resistance (ko01503), and ribosomes (ko03010); the downregulated DEPs were mainly enriched in sulfur metabolism (ko00920), ABC transporters (ko02010), pyruvate metabolism (ko00620) and the pentose phosphate pathway (ko00030). For D120Cr(+) vs. D120Cr(-), the upregulated DEPs were significantly enriched in ribosome (ko03010) and flagellar assembly (ko02040); the downregulated expressed proteins were mainly enriched in tyrosine metabolism (ko00350) and oxidative phosphorylation (ko00190).

The DEPs in all cases were also examined using protein domain enrichment analysis (Figs. 5E and S9). For D120Cr(-) vs. D120N, the DEPs were mainly enriched in RND efflux pump, membrane fusion protein, barrel-sandwich domain; multidrug efflux transporter AcrB TolC docking domain, DN/DC subdomains; and outer membrane protein OmpA-like, transmembrane domain. For D120Cr(+) vs. D120N, the DEPs were significantly enriched in the flagellar basal body rod

protein N-terminal and the TonB-dependent receptor plug domain. For D120Cr(+) vs. D120Cr(-), the DEPs were mainly enriched in the TonB-dependent receptor plug domain, the flagellar basal body rod protein N-terminal, and the TonB-dependent receptor beta-barrel.

The results indicated that the DEPs covered a large range with functions that were categorized into the cellular component, molecular function and biological process. The relevant metabolic pathways were mainly associated with ribosome, flagellar assembly, efflux pump, oxidation resistance, sulfur metabolism, ABC transporters, and energy metabolism. The relevant protein domains were mainly involved in the efflux pump, flagellar, TonB-dependent receptor, and thioredoxin. Furthermore, the enrichment results of upregulation DEPs for D120Cr(+) vs. D120N are similar to that of D120Cr(+) vs. D120Cr(-), while the enrichment results of the downregulated DEPs are similar to that of D120Cr(-) vs. D120N.

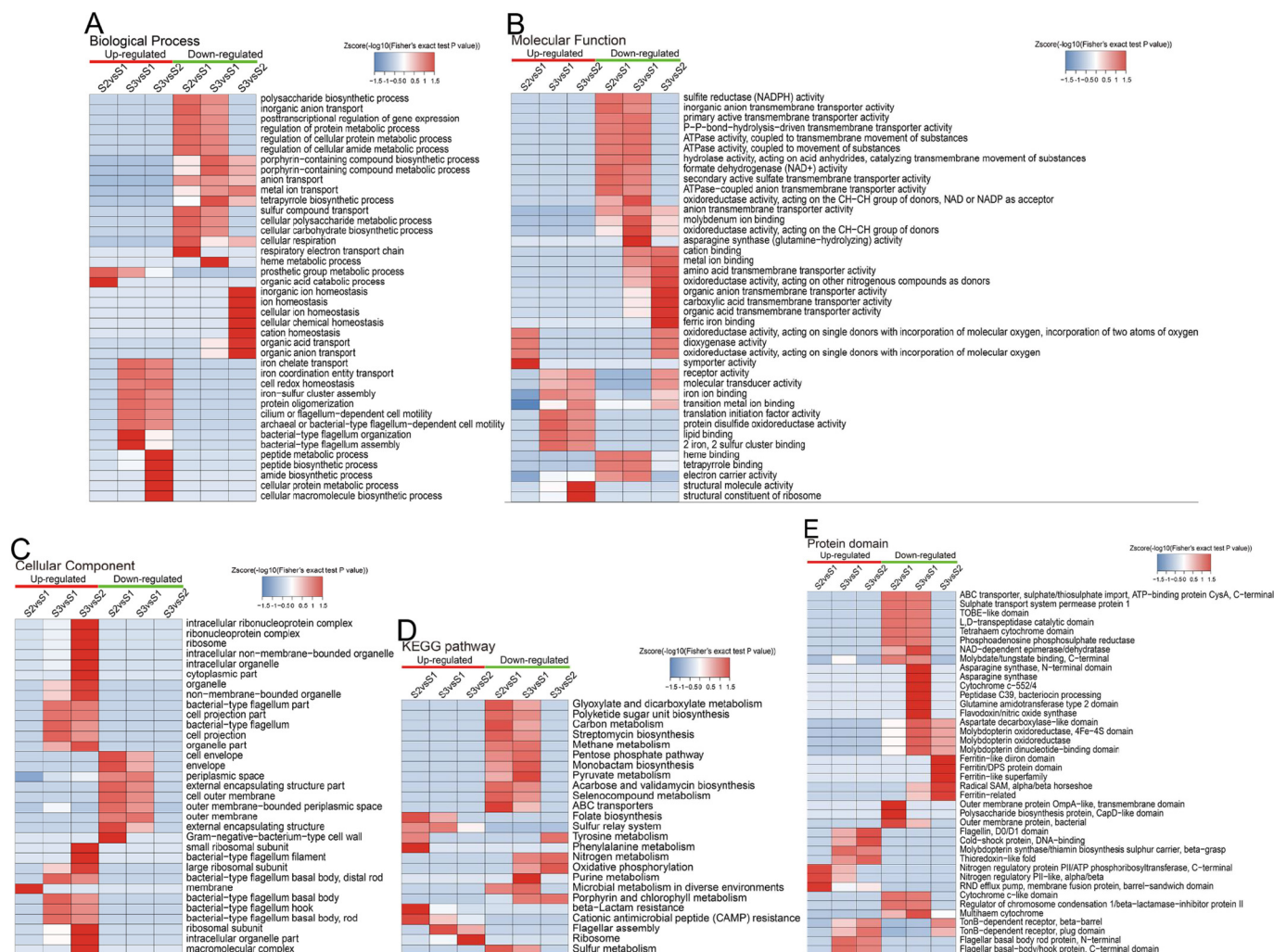


Fig. 5. Hierarchical clustering analysis was conducted for the differentially expressed proteins according to biological process (A), cellular component (B), molecular function (C), protein domain (D) and KEGG pathway (E)-based enrichment. The *P* values were transformed into *Z*-scores for hierarchical clustering analysis. The *Z*-score is shown in the color legend, and the red color represents significant enrichments. S1, D120N; S2, D120Cr(-); S2, D120Cr(+). (For interpretation of the references to this figure legend, the reader is referred to the web version of this article.)

4. Discussion

4.1. Proteome responses to long-term acclimatization under Cr(VI) stress

After a 120-day acclimatization in media with an increasing Cr(VI) concentration, the reduction and resistance capacities of *S. oneidensis* MR-1 to Cr(VI) have been apparently improved (Fig. S10). We investigated the reduction and resistance mechanisms of MR-1 after long-term Cr(VI) exposure at the proteome level by the DEPs for D120Cr(+) versus D120N. The results showed that the long-term Cr(VI) exposure has a remarkable effect on many important biological processes, but proteome could be regulated in response to environmental stress, to some extent.

In contrast to D120N, the abundance of proteins related to structural molecule activity and cell motility, such as the 50S ribosomal protein L31 RpmE, the 30S ribosomal protein S21 RpsU, the flagellar hook-associated protein FlgL, the flagellar hook-filament junction protein FlgK, and flagellin FlhC, were dramatically increased in D120Cr(+). These proteins, which involve the structural molecule activity, contribute to the structural integrity of a complex or its assembly within or outside a cell, especially ribosome. Moreover, the KEGG pathway showed that ribosome at significant enrichment level was the important pathway. Flagellar motility is very important to allow bacteria to move

toward favorable conditions, form biofilms and acquire nutrients (Qin et al., 2011). Wang et al. (2015) found that the flagellar assembly pathway was sensitive to environmental stresses. *S. oneidensis* MR-1 could be benefit-tending and harm-avoiding through the flagellum and motility under long-term Cr(VI) stress. The morphology analysis results also showed that microorganisms tended to aggregate together and occurred in abnormal cell morphologies under Cr(VI) exposure (Fig. S11).

We observed that the thioredoxin-like fold, thioredoxin and glutaredoxin domains involved in the oxidative stress response were increased. When chromate enters a bacterial cell, it leads to the generation of reactive oxygen species and may damage many cellular components (e.g., DNA and proteins) (Cervantes et al., 2001; Singh et al., 1998). And and Storz (2000) proposed that the thioredoxin-dependent reduction systems that were found to be responsible for maintaining the reduction environment of the *Escherichia coli* and *Saccharomyces cerevisiae* cytosol acts as a defense against oxidative stress.

S. oneidensis MR-1 genes/proteins with functions in iron acquisition and homeostasis were up-regulation under acute chromate exposure (Brown et al., 2006; Thompson et al., 2007). Hu et al. (2005) also observed similar results in *Caulobacter crescentus*. Similarly, our result is consistent with the fact that five domains in connection with iron

transport and homeostasis were significantly enriched with upregulated proteins for adapting to the chromate stress environment, namely, the TonB-dependent receptor plug domain, the TonB-dependent receptor beta-barrel, the ferric iron reductase FhuF domain, FeS cluster biogenesis, and the 2Fe–2S ferredoxin-type iron-sulfur binding domain. The TonB-dependent hemoglobin/transferrin/lactoferrin family receptor plays an important role in the cellular adaptation of *Pseudomonas putida* F1 to chromate stress (Thompson et al., 2010). More similar results were reported, *tonB* mutants of *E. coli* K-12 was sensitive to chromium salt, which could be relieved by adding iron to the growth medium (Pugsley and Reeves, 1976; Wang and Newton, 1969). *Pseudomonas stutzeri* KC siderophore pyridine-2,6-bis(thiocarboxylic acid) (pdtc) has been shown to reduce and precipitate Cr(VI), suggesting that a novel role of pdtc was detoxification of extracellular metal toxicity (Zawadzka et al., 2007).

Cr(VI) enters the cells through the sulfate transport system because of the structural similarity of chromate (CrO_4^{2-}) and sulfate (SO_4^{2-}) (Cervantes et al., 2001; Cheung et al., 2006; Nies et al., 1989). Chromate as a competitive inhibitor of sulfate uptake results in low intracellular levels of sulfur (Ohtake et al., 1987). As was expected, the downregulated proteins related to sulfate assimilation and the sulfur metabolism process were significantly enriched in D120Cr(+) in our study. It is a protection strategy that could prevent cells from chromate damage by reducing the absorption to Cr(VI). We have observed that these upregulated proteins that are involved in the sulfur relay system were markedly enriched in D120Cr(+). It may be a compensation mechanism for sulfur absorption to keep enough of the sulfur element for cellular metabolism and normal physiological activities. Thompson et al. (2010) found that the increased uptake of cysteine and cysteine-containing compounds could compensate for the reduced sulfate uptake by other optional transporter systems. In addition, the KEGG pathway showed that CAMP resistance related to the efflux pump at a significant enrichment level was an important pathway for reducing intracellular Cr(VI).

Meanwhile, these downregulated proteins that are associated with pyruvate metabolism and the pentose phosphate pathway were significantly enriched in D120Cr(+); for example, the fumarate reductase FAD-binding subunit FrdA, acetyl-coenzyme A synthetase, the NAD-dependent malic enzyme, D-xylulose 5-phosphate/D-fructose 6-phosphate phosphoketolase Xfp, phosphopentomutase, deoxyribose-phosphate aldolase, and so on. As a consequence, pyruvate metabolism and the pentose phosphate pathway were inhibited in long-term Cr(VI)-treated *S. oneidensis* MR-1, which may be one of the Cr(VI) toxicity mechanisms, and pyruvate and the pentose phosphate pathway may be an important target of Cr(VI) toxicity. Wang et al. (2014) previously reported that Cr(VI) exposure decreased the abundance of proteins that is involved in pyruvate metabolism.

ABC transporters are transmembrane proteins that utilize energy to carry substrates into the cells (Bulut et al., 2012). Our result showed that these proteins related to ABC transporters were decreased and were significantly enriched in D120Cr(+), including the ABC-type sulfate/thiosulfate uptake system substrate-binding subunit Sbp, sulfate/thiosulfate import ATP-binding protein CysA1, sulfate/thiosulfate import ATP-binding protein CysA2, ABC-type sulfate/thiosulfate uptake system substrate-binding component CysP, molybdenum import ATP-binding protein ModC, ABC-type molybdate uptake system substrate-binding component ModA, etc. Karpus et al. revealed that the *E. coli* molybdate-binding protein ModA could bind chromate tightly and was capable of removing chromate (Karpus et al., 2017). These results suggested that the organism could defend Cr(VI) stress by reducing sulfate uptake, and Cr(VI) toxicity has a serious effect on the molybdate transport of MR-1 under long-term Cr(VI) stress.

In summary, D120Cr(+) could better reduce and tolerate long-term Cr(VI) stress in the following aspects: (1) to enhance cell motility and structural integrity, particularly ribosome and flagellar; (2) to promote the oxidative stress response by the thioredoxin-dependent reduction

systems; (3) to maintain iron acquisition and homeostasis for adapting to the chromate stress environment; (4) to enhance efflux by CAMP resistance, and to decrease Cr(VI) uptake by changing sulfate transport system and ABC transporters; (5) to increase the sulfur relay system as a compensation mechanism for sulfur absorption; (6) to weaken energy metabolism, mainly in pyruvate metabolism and the pentose phosphate pathway.

4.2. The permanent effect under long-term Cr(VI) pressure

We could find the permanent changes of MR-1 proteome under long-term Cr(VI) pressure based on the DEPs for D120Cr(–) versus D120N. In the absence of Cr(VI), the D120Cr(–) proteome still had striking changes in some respects; specifically, the efflux pump, amino acid catabolic/metabolic process, dioxygenase activity, oxidoreductase activity, sulfate uptake and reduction, and transport, etc.

Compared with D120N, two key proteins with the function in antioxidant activity have upregulated expressions, namely, homogentisate 1,2-dioxygenase HmgA and 4-hydroxyphenylpyruvate dioxygenase HppD. One of the strategies for detoxifying chromate toxicity is to rapidly extrude it by using the chromate efflux pump from the cytoplasm (Baaziz et al., 2017). These upregulated proteins that are associated with the efflux pump are significantly enriched in beta-lactam resistance, CAMP resistance, the RND efflux pump, the membrane fusion protein, the barrel-sandwich domain and the multidrug efflux transporter AcrB TolC docking domain, and DN/DC subdomains. Specifically, the RND-type multidrug/detergent efflux system MFP component VexB, the RND-type multidrug/detergent efflux system permease component VexA, the efflux pump membrane transporter VmeB, and the proton-coupled multidrug efflux pump MFP component VmeA. Those proteins related to the amino acid catabolic/metabolic processes are also upregulated in D120Cr(–), which could supply more energy for hexavalent chromium reduction and cell growth. It is noteworthy that the phenylalanine metabolic process and tyrosine metabolism are closely related to the synthesis of important neurotransmitters and hormones.

The main biological functions of downregulated proteins for D120Cr(–) versus D120N are similar to that of D120Cr(+) versus D120N, specifically, in transport, sulfur metabolism, and so on. It was indicated that the long-term Cr(VI) treatment could bring about more repressed changes in the above respects, which are permanent in spite of the loss of Cr(VI) stress.

4.3. The proteome responses to short-term Cr(VI) stimulus

Based on the DEPs for D120Cr(+) versus D120Cr(–), we discovered the proteome responses of D120Cr to short-term Cr(VI) stimulus. The enrichment results of the upregulated proteins are similar to that of D120Cr(+) versus D120N, which demonstrates once more that the cellular motility, iron ions and the Fe–S cluster, ribosomes and translation, and antioxidant activity are key factors in the immediate response to Cr(VI) stress. These functions and processes, which are related to the iron ion and the Fe–S cluster, were enhanced, which may be a compensation mechanism for iron ion absorption and Fe–S cluster formation to defend against Cr(VI) stress. The abundance of proteins involved in ribosomes and translation were increased due to Cr(VI) stress. These ribosome-relevant proteins take part in the translation, protein metabolism and RNA process. As a consequence, more proteins are synthesized to maintain the cellular structure and function, to repair damaged proteins and to produce new proteins against Cr(VI) stress. The GO enrichment analysis showed that peptide biosynthetic and metabolic process at significant enrichment levels were enriched by upregulated proteins. It seems to that the short-term Cr(VI) stimulus is more likely to give rise to the upregulated expression of proteins in the above respects.

Wang et al. (2017) observed that Hg treatment inhibited transition

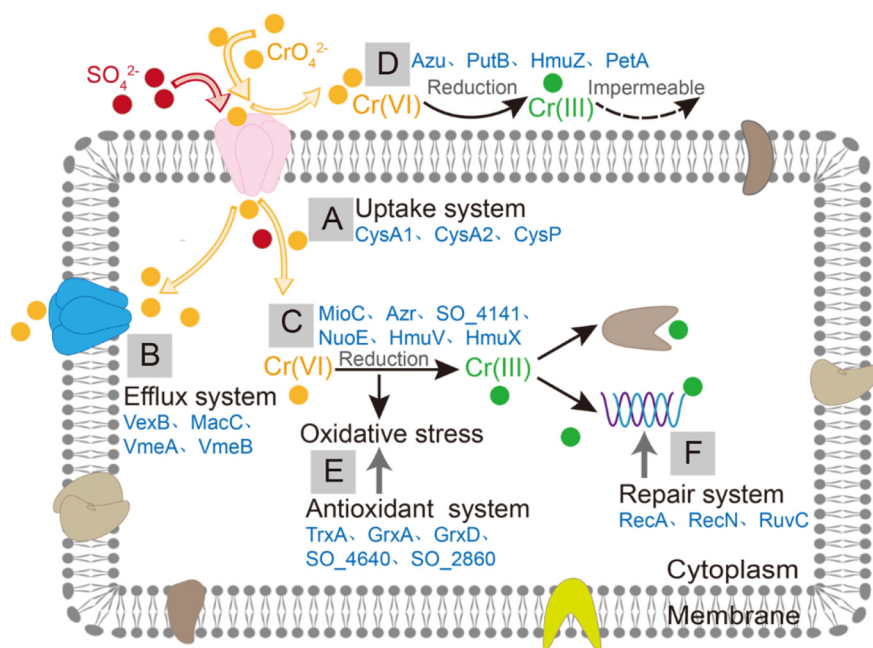


Fig. 6. Mechanisms of chromate resistance and reduction in *S. oneidensis* MR-1 cells. (A) sulfate uptake pathway which is also used by chromate. (B) Efflux of chromate from the cytoplasm. (C) Intracellular reduction of Cr(VI) by chromate reductases. (D) Extracellular reduction of Cr(VI) to Cr(III). (E) Detoxifying enzymes are involved in protection against oxidative stress. (F) DNA repair systems participate in the protection from the damage.

metal binding, iron ion homeostasis and cellular homeostasis. Our study found that both transport and cellular homeostasis were inhibited and significantly enriched with a majority of downregulated DEPs in D120Cr(+). Specifically, organic acid transport, organic anion transport, iron ion transport and homeostasis, and transition metal ion transport homeostasis were inhibited. Two bacterioferritins coded by *brf1* and *brf2*, respectively, were common in all homeostasis processes. It was found that these domains, including the ferritin-like diiron domain, the ferritin/DPS protein domain, the ferritin-like superfamily and the TonB-dependent receptor plug domain, etc., were enriched with downregulated proteins. Hence, it is likely that ferritin is an important target of Cr(VI) toxicity. As previously reported, ferritin exists ubiquitously among living microorganisms; as an iron storage and release protein, it is an important intracellular protein that plays a part in iron metabolism, immune defense, stress response, and so on (Aguilera et al., 2016; Wang et al., 2017). In addition, the inhibition of the transmembrane transporter activity inevitably impacts homeostasis.

Furthermore, two other important pathways were also inhibited; namely, tyrosine metabolism and oxidative phosphorylation. Reactive oxygen species can interact with numerous targets in a microbial cell, including thiols, metal centers, protein tyrosines, nucleotide bases and lipids (Fang, 2004). Moreover, cells could need less ATP to maintain a normal metabolism process under Cr(VI) stress. Therefore, the remarkable depression of those processes suggested that Cr(VI) toxicity leads to dysfunction in the transport and homeostasis of D120Cr(+) due to the damage of several crucial proteins and enzymes.

5. Conclusion

Our study investigated the molecular mechanisms for reduction and resistance of *S. oneidensis* MR-1 under long-term exposure to Cr(VI) by proteomics analysis. In reality, the proteomic changes of *S. oneidensis* MR-1 effected by long-term Cr(VI) acclimatization can be considered to be derived from two aspects: long-term natural growth and Cr(VI) stress. The reduction capacity of *S. oneidensis* MR-1 to Cr(VI) was enhanced mainly in electron transport systems and energy metabolism. The resistance capacity to Cr(VI) was promoted mainly in cellular motility, efflux systems, sulfate transport, sulfur metabolism, oxidative stress protection, and energy metabolism. We summarized the proteins or pathways involved in the Cr(VI) reduction and resistance in bacterial cells (Fig. 6). The Cr(VI) reduction was carried out by intracellular and

extracellular reduction. The Cr(VI) resistance was mainly in uptake, efflux, antioxidant and repair systems. The findings will further shed light on the molecular mechanisms for resistance and reduction in MR-1 under long-term Cr(VI) exposure at the proteomic level, which could help us to make effective bioremediation and environmental risk assessments through long-term acclimatization. Further studies can be conducted for Cr(VI) bioremediation: (1) to investigate deeply certain key proteins/genes and their interaction networks; (2) to optimize or develop environmental microbial technologies, e.g. strain modification and the change of domestication strategy; (3) to prevent and control the harmful microorganisms from Cr(VI)-contaminated environments.

Acknowledgements

This study was supported by grants from the National Natural Science Foundation of China (51878640, 51478451) and the Youth Innovation Promotion Association of Chinese Academy of Sciences (2018344).

Appendix A. Supplementary data

Supplementary data to this article can be found online at <https://doi.org/10.1016/j.envint.2019.03.016>.

References

- Aguilera, V.M., Vargas, C.A., Lardies, M.A., Poupin, M.J., 2016. Adaptive variability to low-pH river discharges in *Acartia tonsa* and stress responses to high PCO₂ conditions. *Mar. Ecol.* 37, 215–226.
- Alencar, F.L.S.D., Navoni, J.A., Amaral, V.S.D., 2017. The use of bacterial bioremediation of metals in aquatic environments in the twenty-first century: a systematic review. *Environ. Sci. Pollut. Res. Int.* 24, 1–15.
- And, C.H., Storz, G., 2000. Roles of the glutathione- and thioredoxin-dependent reduction systems in the *Escherichia Coli* and *Saccharomyces Cerevisiae* responses to oxidative stress. *Annu. Rev. Microbiol.* 54, 439–461.
- Baaziz, H., Gambari, C., Boyeldieu, A., Chaoche, A.A., Alatou, R., Mejean, V., et al. 2017. ChrA(SO), the chromate efflux pump of *Shewanella oneidensis*, improves chromate survival and reduction. *PLoS One*, 12, 15.
- Belchik, S.M., Kennedy, D.W., Dohnalkova, A.C., Wang, Y., Sevinc, P.C., Wu, H., et al. 2011. Extracellular reduction of hexavalent chromium by cytochromes MtrC and OmcA of *Shewanella oneidensis* MR-1. *Appl. Environ. Microbiol.*, 77, 4035–4041.
- Bencheikh-Latmani, R., Williams, S.M., Haucke, L., Criddle, S.C., Wu, L., 2005. Global transcriptional profiling of *Shewanella oneidensis* MR-1 during Cr(VI) and U(VI) reduction. *Appl. Environ. Microbiol.* 71, 7453–7460.
- Brown, S.D., Thompson, M.R., Verberkmoes, N.C., Chourey, K., Shah, M., Zhou, J., et al.

2006. Molecular dynamics of the *Shewanella oneidensis* response to chromate stress. *Mol. Cell. Proteomics*, 5, 1054–1071.
- Bulut, H., Moniot, S., Licht, A., Scheffel, F., Gathmann, S., Saenger, W., et al. 2012. Crystal structures of two solute receptors for L-cystine and L-cysteine, respectively, of the human pathogen *Neisseria gonorrhoeae*. *J. Mol. Biol.*, 415, 560–572.
- Cervantes, C., Campos-García, J., Devars, S., Gutierrez-Corona, F., Loza-Tavera, H., Torres-Guzman, J.C., et al. 2001. Interactions of chromium with microorganisms and plants. *FEMS Microbiol. Rev.*, 25, 335–347.
- Chai, L.Y., Yang, Z.H., Shi, Y., Liao, Q., Min, X.B., Li, Q.Z., et al. 2018. Cr (VI)-reducing Strain and Its Application to the Microbial Remediation of Cr (VI)-contaminated Soils.
- Chen, Y., Liu, Y., Zhou, Q., Gu, G., 2006. Enhanced phosphorus biological removal from wastewater—effect of microorganism acclimatization with different ratios of short-chain fatty acids mixture. *Biochem. Eng. J.* 27, 24–32.
- Cheung, K.H., Gu, J.D., 2007. Mechanism of hexavalent chromium detoxification by microorganisms and bioremediation application potential: a review. *Int. Biodeterior. Biodegrad.* 59, 8–15.
- Cheung, K.H., Lai, H.Y., Gu, J.D., 2006. Membrane-associated hexavalent chromium reductase of *Bacillus megaterium* TKW3 with induced expression. *J. Microbiol. Biotechnol.* 16, 855–862.
- Dhal, B., Thatoi, H.N., Das, N.N., Pandey, B.D., 2013. Chemical and microbial remediation of hexavalent chromium from contaminated soil and mining/metallurgical solid waste: a review. *J. Hazard. Mater.* 250–251, 272–291.
- Fang, F.C., 2004. Antimicrobial reactive oxygen and nitrogen species: concepts and controversies. *Nat. Rev. Microbiol.* 2, 820–832.
- Hu, P., Brodie, E.L., Suzuki, Y., Mcadams, H.H., Andersen, G.L., 2005. Whole-genome transcriptional analysis of heavy metal stresses in *Caulobacter crescentus*. *J. Bacteriol.* 187, 8437–8449.
- Karpus, J., Bosscher, M., Ajiboye, I., Zhang, L., He, C., 2017. Chromate binding and removal by the molybdate-binding protein ModA. *Chembiochem* 18, 633–637.
- Meng, Y., Zhao, Z., Burgos, W.D., Li, Y., Zhang, B., Wang, Y., et al. 2018. Iron(III) minerals and anthraquinone-2,6-disulfonate (AQDS) synergistically enhance bioreduction of hexavalent chromium by *Shewanella oneidensis* MR-1. *Sci. Total Environ.*, s 640–641, 591–598.
- Nies, A., Nies, D.H., Silver, S., 1989. Cloning and expression of plasmid genes encoding resistances to chromate and cobalt in *Alcaligenes eutrophus*. *J. Bacteriol.* 171, 5065–5070.
- Ohtake, H., Cervantes, C., Silver, S., 1987. Decreased chromate uptake in *Pseudomonas fluorescens* carrying a chromate resistance plasmid. *J. Bacteriol.* 169, 3853–3856.
- Pradhan, D., Sukla, L.B., Sawyer, M., Rahman, P.K.S.M., 2017. Recent bioreduction of hexavalent chromium in wastewater treatment: a review. *J. Ind. Eng. Chem.* 55, 1–20.
- Pugsley, A.P., Reeves, P., 1976. Iron uptake in colicin B-resistant mutants of *Escherichia coli* K-12. *J. Bacteriol.* 126, 1052–1062.
- Qin, Q.L., Li, Y., Zhang, Y.J., Zhou, Z.M., Zhang, W.X., Chen, X.L., et al. 2011. Comparative genomics reveals a deep-sea sediment-adapted life style of *Pseudalteromonas* sp. SM9913. *ISME J.*, 5, 274–284.
- Singh, J., Carlisle, D.L., Pritchard, D.E., Patierno, S.R., 1998. Chromium-induced genotoxicity and apoptosis: relationship to chromium carcinogenesis (review). *Oncol. Rep.* 5, 1307–1318.
- Thompson, D.K., Chourey, K., Wickham, G.S., Thieman, S.B., Verberkmoes, N.C., Zhang, B., et al. 2010. Proteomics reveals a core molecular response of *Pseudomonas putida* F1 to acute chromate challenge. *BMC Genomics*, 11, 311.
- Thompson, M., Verberkmoes, N., Chourey, K., Shah, M., Thompson, D., Hettich, R., 2007. Dosage-dependent proteome response of *Shewanella oneidensis* MR-1 to acute chromate challenge. *J. Proteome Res.* 6, 1745–1757.
- Wang, C., Chen, J., Hu, W.J., Liu, J.Y., Zheng, H.L., Zhao, F., 2014. Comparative proteomics reveal the impact of OmcA/MtrC deletion on *Shewanella oneidensis* MR-1 in response to hexavalent chromium exposure. *Appl. Microbiol. Biotechnol.* 98, 9735–9747.
- Wang, C., Deng, H., Zhao, F., 2016. The remediation of chromium (VI)-contaminated soils using microbial fuel cells. *J. Soil Contam.* 25, 1–12.
- Wang, C.C., Newton, A., 1969. Iron transport in *Escherichia coli*: relationship between chromium sensitivity and high iron requirement in mutants of *Escherichia coli*. *J. Bacteriol.* 98, 1135–1141.
- Wang, L., Huang, L.X., Su, Y.Q., Qin, Y.X., Kong, W.D., Ma, Y., et al. 2015. Involvement of the flagellar assembly pathway in *Vibrio alginolyticus* adhesion under environmental stresses. *Front. Cell. Infect. Microbiol.*, 5, 59.
- Wang, M.H., Lee, J.S., Li, Y., 2017. Global proteome profiling of a marine copepod and the mitigating effect of ocean acidification on mercury toxicity after multi-generational exposure. *Environ. Sci. Technol.* 51, 5820–5831.
- Wang, Y.T., Shen, H., 1995. Bacterial reduction of hexavalent chromium. *J. Ind. Microbiol.* 14, 159–163.
- Yang, N., Wan, J.F., Zhao, S.J., Wang, Y., 2015. Removal of concentrated sulfamethazole by acclimatized aerobic sludge and possible metabolic products. *PeerJ* 3, 15.
- Zawadzka, A.M., Crawford, R.L., Paszczynski, A.J., 2007. Pyridine-2,6-bis(thiocarboxylic acid) produced by *Pseudomonas stutzeri* KC reduces chromium(VI) and precipitates mercury, cadmium, lead and arsenic. *Biometals* 20, 145–158.